# MEASUREMENT OF AIRFOIL HEAT TRANSFER COEFFICIENTS ON A TURBINE STAGE*

Robert P. Dring, Michael F. Blair, and H. David Joslyn
United Technologies Research Center
East Hartford, Connecticut

The Primary basis for heat transfer analysis of turbine airfoils is experimental data obtained in linear cascades. These data have been very valuable in identifying the major heat transfer and fluid flow features of a turbine airfoil. The question of major interest is how well all of these data translate to the rotating turbine stage. It is suggested from the work of Lokay and Trushin (ref. 1) that average heat transfer coefficients on the rotor may be as much as 40 percent above the values measured on the same blades nonrotating. Recent work by Dunn and Holt (ref. 2) supports the conclusion of reference 1. What is needed is a set of data from a rotating system which is of sufficient detail as to make careful local comparisons between static cascade and rotor blade heat transfer. In addition, data is needed in a rotating system in which there is sufficient documentation of the flow field to support the computer analyses being developed today. Other important questions include the impact of both random and periodic unsteadiness on both the rotor and stator airfoil heat transfer. The random unsteadiness arises from stage inlet turbulence and wake generated turbulence and the periodic unsteadiness arises from blade passing effects. A final question is the influence, if any, of the first stator row and first stator inlet turbulence on the heat transfer of the second stator row after the flow has been passed through the rotor.

## OBJECTIVES

The first program objective is to obtain a detailed set of heat transfer coefficients along the midspan of a stator and a rotor in a rotating turbine stage. These data are to be such that the rotor data can be compared directly with data taken in a static cascade. The data are to be compared to some standard analysis of blade boundary layer heat transfer which is in use today. In addition to providing this all-important comparison between rotating and stationary data, this experiment should provide important insight to the more elaborate full three-dimensional programs being proposed for future research. A second program objective is to obtain a detailed set of heat transfer

*Work done under NASA Contract NAS3-23717.

coefficients along the midspan of a stator located in the wake of an upstream turbine stage. Particular focus here is on the relative circumferential location of the first and second stators. Both program objectives will be carried out at two levels of inlet turbulence. The low level will be on the order of 1 percent while the high level will be on the order of 10 percent which is more typical of combustor exit turbulence intensity. The final program objective is to improve the analytical capability to predict the experimental data.

## DESCRIPTION OF EXPERIMENTAL EQUIPMENT AND TEST CONDITIONS

The experimental portion of this study was conducted in a large-scale (aproximately 5x engine), ambient temperature, rotating turbine model configured in both single-stage and stage-and-a-half arrangements. Heat transfer measurements were obtained using low-conductivity airfoils with miniature thermocouples welded to a thin, electrically heated surface skin. Heat transfer data were acquired for various combinations of low or high inlet turbulence intensity, flow coefficient, first-stator/rotor axial spacing, Reynolds number and relative circumferential position of the first and second stators. High levels of inlet turbulence were generated using a coarse biplane grid located 2 1/2 axial chords upstream of the first stator leading edge plane. With the grid out the midspan region turbulence intensity was slightly greater than 1/2% with much higher levels in the endwall boundary layers. With the grid in the midspan turbulence intensity averaged 9.8%. Spectral measurements of the grid generated turbulence indicated that it was in excellent agreement with the von Karman isotropic spectrum. Aerodynamic measurements obtained as part of the program include distributions of the mean and fluctuating velocities at the turbine inlet and, for each airfoil row, midspan airfoil surface pressures and circumferential distributions of the downstream steady state pressure and fluctuating velocities.

## RESULTS

In-depth descriptions of the results of this program have already been presented at previous HOST contractor reviews. These descriptions have covered: (1) the heat transfer measurement technique, (2) both the turbulence and the time averaged nature of the flow entering the turbine model, (3) the effects of Reynolds number on the single-stage stator and rotor heat transfer, (4) the effects of inlet free-stream turbulence on the single-stage stator and rotor heat transfer, (5) the effects of stator/rotor axial spacing on the single-stage stator and rotor heat transfer, (6) the effects of extreme incidence variation on the rotor heat transfer, (7) the effect of the relative circumferential position of the first stator on the second stator heat transfer, (8) the nature of the heat transfer in the stagnation region of each airfoil, and (9) a comparison of the heat transfer for the rotor with the same airfoil midspan geometry in a plane cascade. The present discussion will focus on experimental/analytical comparisons for the first and second stators and for the rotor, and on the heat transfer trends from a surface averaged

point of view. Distributions of heat transfer along the various airfoil surfaces are presented as Stanton numbers based on exit conditions vs dimensionless surface distance. Included in figures 1, 2 and 3 are the specific flow coefficient and axial spacing for the data set and a note indicating whether the turbulence grid was IN or OUT.

The boundary layer analysis chosen for the present assessment is the "ABLE" code of Carter, Edwards and Werle (refs. 3 and 4). This is an efficient and versatile calculation that includes models for laminar, transitional, and turbulent flow. The ABLE code contains a number of options for the transition and turbulence models that are employed. In the present assessment two such models have been evaluated. The first was the algebraic turbulence model of Cebeci and Smith (ref. 5). The other model that will be evaluated is that of McDonald et al. (refs. 6 and 7). This analysis includes physical models for both transitional and turbulent flow, both of which are functions of the free-stream turbulence imposed. With this model the level of free-stream turbulence controls both the onset and the length of transition. It should be pointed out, however, that the turbulent Prandtl number profile used in the present comparison was not that of McDonald and Kreskovsky (ref. 7) but rather a profile based on the measurements of Blair (ref. 8) was used in its place. The effect of this modified turbulent Prandtl number profile was to increase the predicted Stanton numbers slightly beginning in the transitional region and through the turbulent region. The increase was typically 6% in the turbulent region.

The analytical/experimental comparisons for this assessment are shown in figures 1, 2, and 3 for the first stage stator, rotor, and the second stage stator respectively. The comparisons are all for the 0.78 flow coefficient. Comparisons were also made at 0.68 and 0.96 but the conclusions drawn were no different than those at 0.78. The comparisons are all for the data acquired in the 65% axial gap configuration. Changing the axial gap from 15% to 65% had little effect on the measured results. All of the comparisons are for the high Reynolds number cases, i.e. Reynolds numbers in the range of 600,000. Finally, the comparisons are with the data acquired both with the grid in and with the grid out. With the grid out the stage inlet turbulence was 0.5% and with the grid in it was typically 10%. Each of the figures includes a laminar prediction up to laminar separation indicated by "L", a fully turbulent prediction (using the Cebeci and Smith model, ref. 5) indicated by "T", and a family of transitional predictions (using the model of McDonald and Kreskovsky, ref. 7 with the turbulent Prandtl number profile of Blair, ref. 8) indicated by the level of the free-stream turbulence used in each calculation. On the pressure surfaces the transitional predictions for free-stream turbulences up to 10% were generally very close to the laminar predictions. On the suction surfaces increasing the free-stream turbulence produced a monotonic upstream movement of transition.

On the pressure surfaces of the three airfoils reasonable agreement between the measured and the computed results was only obtained on the first stator with the grid out. With the grid in the measured data were far above even the fully turbulent prediction. Similarly the pressure surface data for the rotor and the second stator were far above the fully turbulent predictions for the grid both in and out. It was previously observed that these high

pressure surface Stanton numbers occurred when the inlet unsteadiness was high (due to either turbulence or the passing of an upstream airfoil row) and when the Reynolds number was high. At lower Reynolds numbers the Stanton numbers reduced to near the fully turbulent level.

On the suction surfaces of the three airfoils the agreement between the measured and computed results was genrally unsatisfactory for both the cases with the grid in and with the grid out. The best agreement was obtained on the rotor for the case with the grid in. In this case after transition the data were in good agreement with the fully turbulent prediction. On the first stator the transition predictions were in poor agreement with the data in spite of the relatively benign inflow condition, i.e. without an upstream airfoil row. On the rotor the transition predictions were also poor. This may be related to the wakes of the upstream stator but recall that the rotor Stanton number distribution varied only slightly as the stator/rotor axial gap was changed from 15% to 65% with the grid both out and in. The analytical/experimental agreement for the second stator is poor but this is at least in part due to three dimensional effects present in the flow over the airfoil.

The results have also been examined in terms of the average Stanton number on the suction surface, on the pressure surface, and around the entire airfoil. These results are presented in figures 4 through 7 in terms of the variation of the average Stanton number with Reynolds number (based on axial chord and airfoil exit flow velocity). All of the averaged data shown here is for the case of the turbine operating at its design flow coefficient ($C_x/U_m$=0.78), and with the rotor/stator axial spacing equal to 15%.

Figure 4 illustrates the results for the first stator with the grid out. Suction (S) and pressure (P) surface data are shown as the symbols along with the fully turbulent (T) and laminar (L) predictions. The laminar prediction is shown only for the pressure surface. With the grid out the pressure surface is in good agreement with the laminar prediction. This could also be seen in figure 1. On the suction surface, however, because of the long region of laminar flow prior to transition (see fig. 1), the measured results are 30% below the fully turbulent prediction.

Figure 5 illustrates the results for the first stator with the grid in. These results are significantly different from those with the grid out (fig. 4). The data on both the suction and pressure surfaces are much closer to the fully turbulent predictions. The trends with Reynolds number, however, are particularly noteworthy. With the grid out (fig. 4) the Reynolds number trends were very similar to the laminar and turbulent predictions. With the grid in (fig. 5) there is a rising trend with increasing Reynolds number, especially on the pressure surface. At the highest Reynolds number the average pressure surface Stanton number is 40% greater than the fully turbulent prediction.

Figure 6 illustrates the results for the rotor with the grid both out and in. The suction and pressure surface data are shown in comparison with fully turbulent predictions and with the cascade data of Graziani et al. (ref. 9) for this same rotor midspan geometry. Several things are evident in this comparison. First, the difference between the grid in and grid out results is

much less than for the first stator due to the presence of the stator wakes passing over the rotor. Second, the trend of increasing Stanton number with increasing Reynolds number is even stronger on the rotor pressure surface than on the stator and it is occurring with the grid both in and out. At the highest Reynolds number with the grid in the average pressure surface Stanton number is 80% greater than the fully turbulent prediction (and 50% higher with the grid out). Finally, it can also be seen that the cascade results are consistent with the rotating rig results when the differences in Reynolds number and inlet turbulence (unsteadiness) are accounted for.

Figure 6 also illustrates the results for the rotor with the grid both out and in. The results shown here are for the average around the entire airfoil (suction and pressure surfaces). The figure includes the fully turbulent prediction, the cascade data of Graziani et al. (ref. 9), and the data of Lokay and Trushin (ref. 1, fig. 3). Several things are apparent. First, the differences in Reynolds number and inlet turbulence (unsteadiness) are sufficient to reconcile the present rotating rig results with the cascade results. Second, the typically 40% difference between the rotating and stationary results of Lokay and Trushin may also be due to inlet turbulence and unsteadiness. There is no evidence in the present results that this difference is in any way related to the effects of rotation (e.g. Coriolis or centrifugal effects). Some caution should be taken with regard to the data of Lokay and Trushin (ref. 1) due to the rather low Reynolds numbers at which they operated. Boundary layer separation may have been present.

## CONCLUSIONS

A combined experimental and analytical program has been conducted to examine the impact of a number of variables on the midspan heat transfer coefficients of the three airfoil rows in a one and one-half stage large scale turbine model. These variables included:

- o stator 1/rotor axial spacing (15% and 65%)
- o Reynolds number (flow speed)
- o turbine inlet turbulence (0.5% and 10%)
- o flow coefficient (airfoil incidence)
- o relative stator 1/stator 2 circumferential position
- o rotation (rotor vs. cascade)

Heat transfer data were acquired on the suction and pressure surfaces of the three airfoils. High density data were also acquired in the leading edge stagnation regions. In addition to the heat transfer data, extensive documentation of the steady and unsteady aerodynamics was also acquired. Finally, the heat transfer data were compared with both a steady and an unsteady boundary layer analysis. Specific conclusions in each of these areas were as follows:

## Steady Aerodynamics

It was observed that the airfoil midspan pressure distributions were in good agreement with two dimensional potential flow and that they were essentially unaffected by either the turbulence generating grid or the axial gaps between the airfoil rows. It was also observed that the turbulence generating grid had no significant impact on the circumferential distributions of flow speed downstream of each row of airfoils. The conclusion reached here was that the midspan aerodynamics in this experiment were well behaved and that the heat transfer results would be typical of those of a well-designed turbine.

## Unsteady Aerodynamics

It was observed that the turbulence generating grid produced the desired level of turbine inlet turbulence (approximately 10%) and that the grid produced a large increase in total unsteadiness at the first stator exit. At the rotor exit and at the second stator exit, however, the change in unsteadiness level due to the grid was insignificant. The major conclusion reached here was that combustor-generated unsteadiness would strongly affect the flow over the first sttor of a turbine but that downsteam rows would be dominated by turbine-generated unsteadiness.

## Heat Transfer

It was observed that a combination of unsteadiness, high Reynolds number and concave curvature could produce pressure surface heat transfer distributions well in excess of fully turbulent levels. It was shown that boundary layer separtion could also cause large increases in heat transfer. Finally, it was demonstrated that while turbine inlet turbulence can have a very strong impact on the first stator heat transfer, its impact on downstream rows is minimal. The major conclusion reached here was that pressure surface heat transfer could be well in excess of design predictions due to both combustor- and turbine-generated unsteadiness and that this is an area where additional research is sorely needed.

## Steady Boundary Layer Analysis

The boundary layer transition and turbulence models examined in this assessment did not provide accurate predictions of either the transitional nature of the suction surface boundary layers or the very high heat transfer observed on the pressure surfaces. Although only one transition and turbulence model was assessed here the major conclusion is consistent with many previous assessments of other models. This conclusion is that these models are not yet capable of consistently predicting many of the important features of the heat transfer on turbine airfoils and that actual engine designs will probably have to rely, at least in part, on a correlative approach.

## Unsteady Boundary Layer Analysis

An unsteady, compressible boundary layer analysis was developed to study the effects of rotor/stator interaction on the heat transfer rate at the blade surfaces. This analysis was applied to the present rotor/stator configuration using the measured pressure distributions as input to the boundary layer calculations. The conclusion drawn for these calculations was that the time averaged effect of unsteadiness on heat transfer was small since the time average of the unsteady heat transfer predictions differed only slightly from the heat transfer calculated for a steady prediction.

## REFERENCES


1. Lokay, V. I., and Trushin, V. A.: Heat Transfer from the Gas and Flow-Passage Elements of a Rotating Gas Turbine. Heat Transfer-Soviet Research, Vol. 2, No. 4, July 1970.

2. Dunn, M. G., and Holt, J. L.: The Turbine Stage Heat Flux Measurements. Paper No. 82-1289, AIAA/ASME 18th Joint Propulsion Conference, Cleveland, Ohio, June 21-23, 1982.

3. Carter, J. E., Edwards, D. E. and Werle, M. J.: Coordinate Transformation for Laminar and Turbulent Boundary Layers, AIAA Journal, Vol. 20, No. 2, February 1982, pp. 282-284.

4. Edwards, D. E., Carter, J. E. and Werle, M. J.: Analysis of the Boundary Layer Equations Including a Coordinate Transformation--The ABLE Code, UTRC 81-30, 1981.

5. Cebeci, T. and Smith, A. M. O.: Analysis of Turbulent Boundary Layers, Academic Press, 1974.

6. McDonald, H. and Fish, R. W.: Practical Calculation of Transitional Boundary Layer. International Journal of Heat and Mass Transfer, Vol. 16, No. 9, 1973, pp. 1729-1744.

7. McDonald, H. and Kreskovsky: Effect of Free-Stream Turbulence on the Turbulent Boundary Layer, International Journal of Heat and Mass Transfer, Vol. 17, 1974.

8. Blair, M. F. and Edwards, D. E.: The Effects of Free-Stream Turbulence on the Turbulence Structure and Heat Transfer in Zero Pressure Gradient Boundary Layers, Final Report for AFOSR Contract No. F49620-81-C-0053, AFOSR TR-83-0149, Gov't Acc. No. ADA 126465, November 1982.

9. Graziani, R. A., M. F. Blair, J. R. Taylor and R. E. Mayle: An Experimental Study of Endwall and Airfoil Surface Heat Transfer in a Large Scale Turbine Blade Cascade, ASME Journal of Eng. for Power, Vol. 102, April 1980, pp. 257-267.

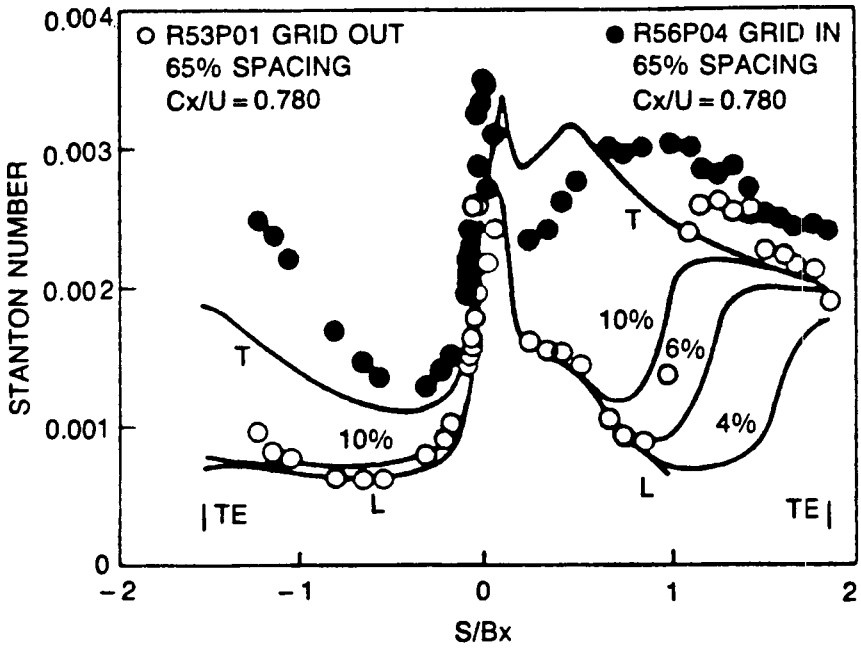


**Fig. 1. Analytical/experimental comparisons for the first stage stator, Cx/U = 0.78.**

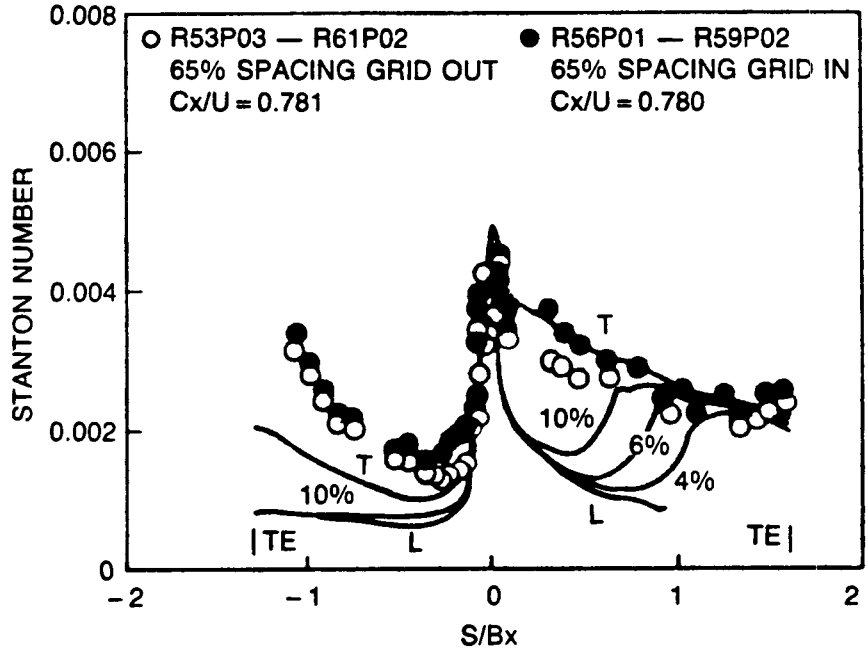


**Fig. 2. Analytical/experimental comparisons for the first stage rotor, Cx/U = 0.78.**

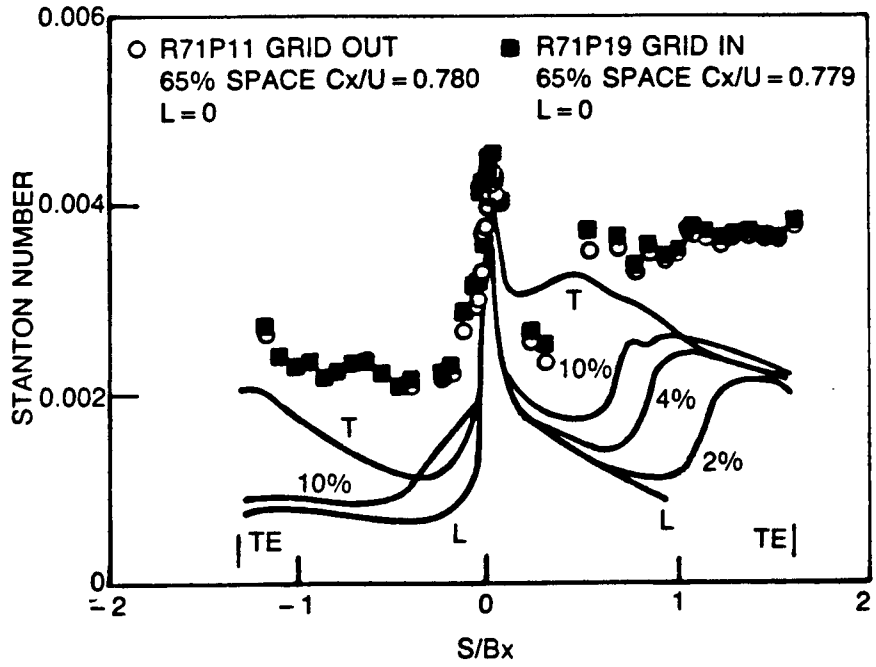


**Fig. 3. Analytical/experimental comparisons for the second stage stator, Cx/U = 0.78.**

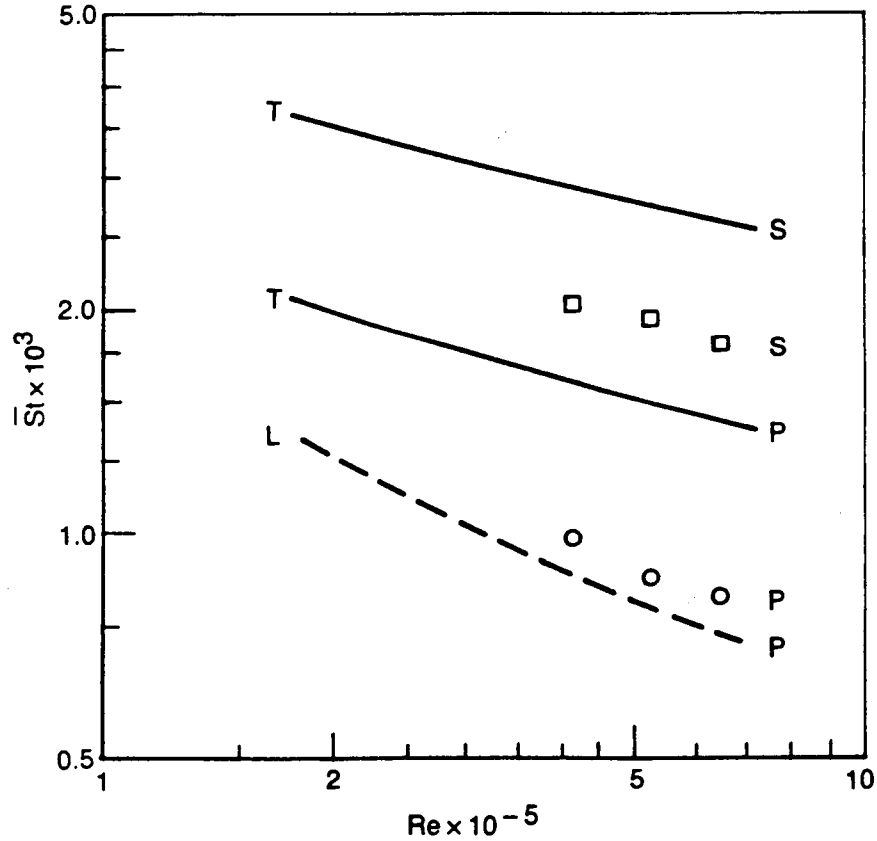


**Fig. 4. First stator averaged suction (S) and pressure (P) surface heat transfer, $\phi = 0.78$, 15% gap, grid out.**

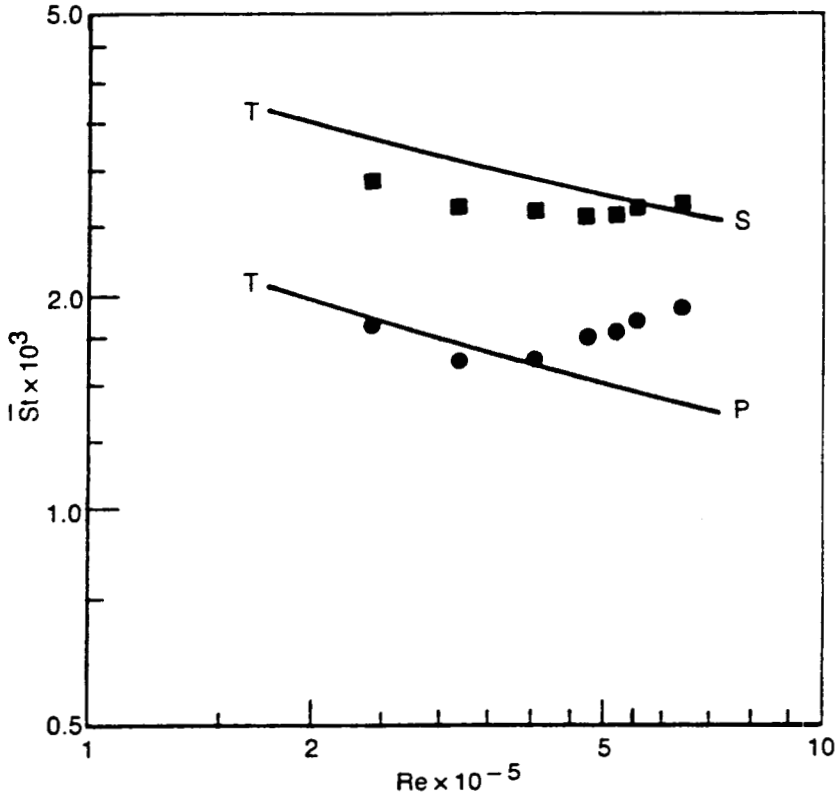


**Fig. 5. First stator averaged suction (S) and pressure (P) surface heat transfer, $\phi = 0.78$, 15% gap, grid in.**

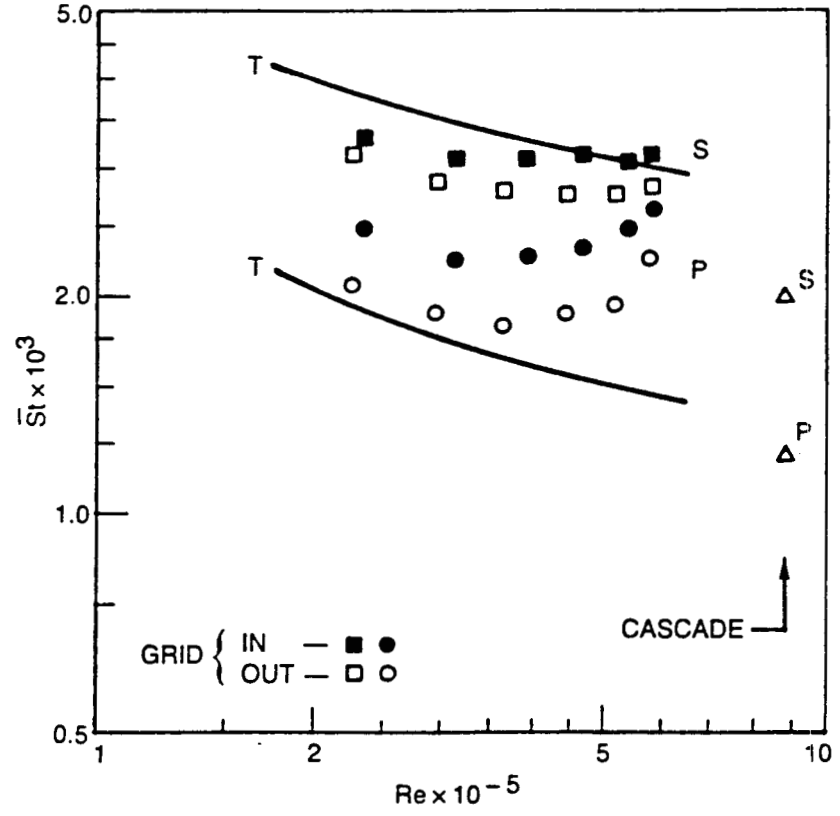


**Fig. 6. Rotor averaged suction (S) and pressure (P) surface heat transfer, $\phi = 0.78$, 15% gap, grid in and out.**

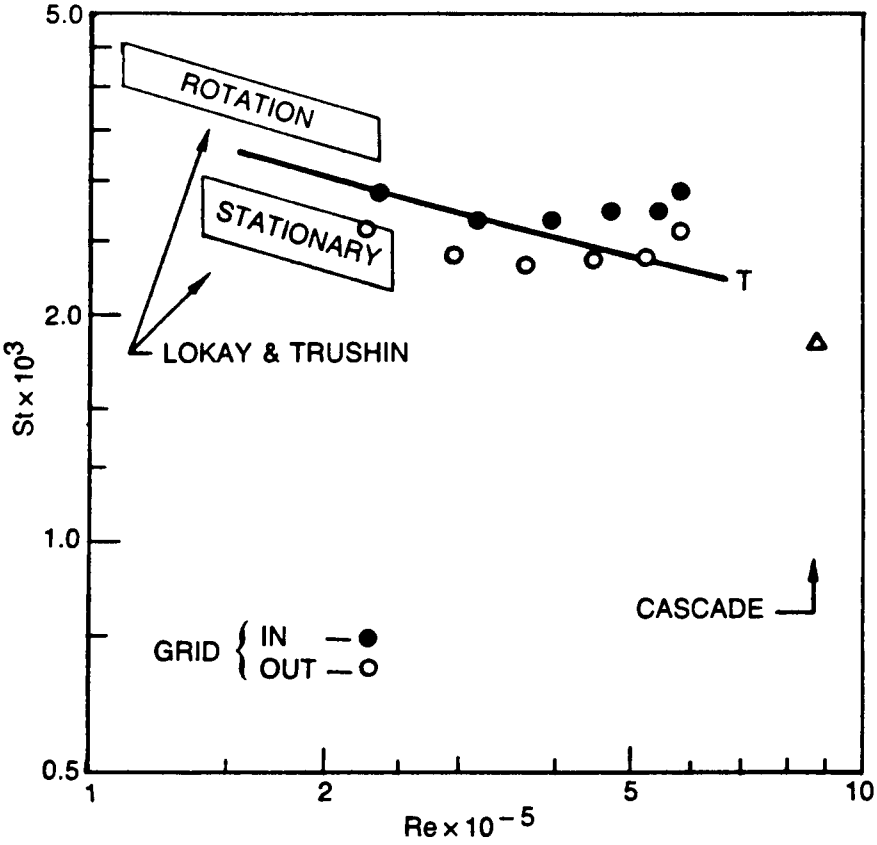


**Fig. 7. Rotor averaged airfoil heat transfer, $\phi = 0.78$, 15% gap, grid in and out.**